



WP4 D4.3 D11

**Report on process-based geophysical
methodologies to monitoring subsurface
processes**

DECEMBER 2019 - Scientific deliverable
Enigma ITN

WP4 - Create new methods for tracking the transport and reactivity of chemical species in subsurface

D4.3/ D11: Report on process-based geophysical methodologies to monitoring subsurface processes

Estimated delivery date: 31/12/2019 - Delivery date: 13/11/2019

Lead Beneficiary:

University of Lausanne: Niklas Linde (Senior manager of this deliverable)

Contributors for this report:

Jülich Forschungszentrum: Satoshi Izumoto (ESR12), Peleg Haruzi (ESR10)

University of Lausanne: Alejandro Fernandez Visentini (ESR9)

University of Liège: Richard Hoffmann (ESR11)

Objectives of this work package

The objective of WP4 is to expand our capability to monitor transport and reaction processes in the subsurface. This work package is currently providing laboratory and in-situ datasets to improve conceptual models, particularly to avoid the common situation in which lab experiments and borehole measurements of chemical species concentrations do not well represent in-situ concentrations. The main challenge is to obtain probabilistic estimates of concentration and reaction rate distributions, while coping with the limited spatial resolutions of imaging techniques and the multiple sources of signals associated with transport and reaction processes. This overall theme of the work package is illustrated in Figure 1.

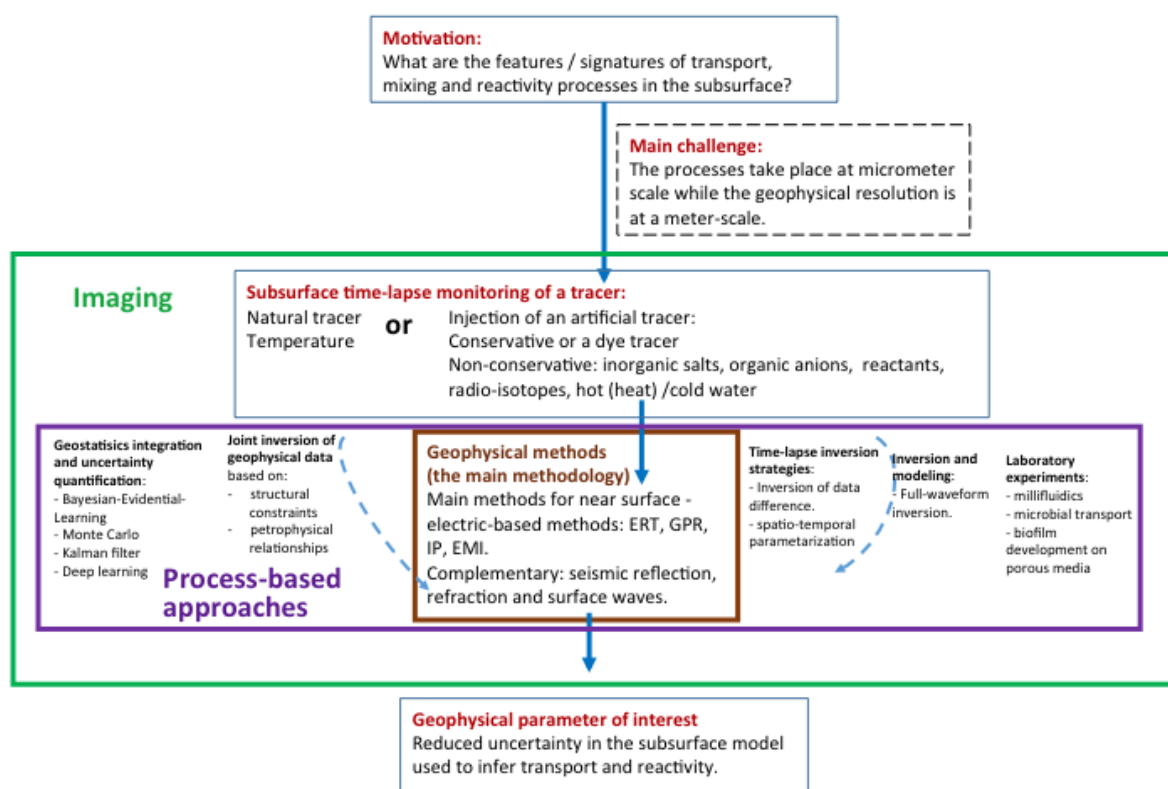


Figure 1: Overall flow chart demonstrating the topics and challenges faced in this report.

Description of work

The identified activities are to (i) develop an upscaling framework for quantifying the impact of spreading and mixing on geophysical signals (ESR9), (ii) develop quantitative inversion of SIP signals induced by biochemical processes (ESR12) and (iii) enhance resolution of time lapse geophysical imaging of transport with new experimental and inversion strategies (ESR10, ESR11). In the following report, we start by discussing the ongoing laboratory experiments and associated theoretical developments (ESR9 and 10), before moving to crosshole time-lapse GPR (ESR10) and finally to the use of innovative traces (ESR11) to image transport processes. In this way, we will naturally move

from the pore scale and the scale of representative elementary volumes (REV), to metric scale and finally to larger field scales.

Introduction and literature review

In this introductory section, the emphasis is placed on a literature review with emphasis on the scientific challenges and scientific opportunities pertaining to the themes of the four ESR (ESR9-12) projects. Narrowing down the scope in this way allows for a fair assessment of the current progress.

Sub-resolution effects on upscaled electrical properties

Time-lapse Direct Current (DC) measurements are commonly used in combination with saline hydrogeological tracer tests to enhance our ability to make inferences about hydrological flow and transport properties compared with what is possible using hydrogeological data alone. Multiple time-lapse DC data enable time-lapse Electrical Resistivity Imaging (ERI), which uses the acquired data to invert for time-varying electrical properties represented in terms of inversion images (tomograms). Researchers commonly transform these images into maps of solute concentrations that evolve over time. From this information, transport parameters and state variables such as mean plume velocity and dispersion can be estimated. Time-lapse ERI has been used to calibrate Advection Dispersion Equation (ADE) parameters in controlled experiments (e.g., Vanderborght et al., 2005; Koestel et al., 2008; Camporese et al., 2011) and in field experiments (Binley et al., 2002; Singha and Gorelick, 2005; Cassiani et al., 2006; Monego et al., 2010; Doetsch et al., 2012; Briggs et al., 2013). The DC method has also been shown to yield clear signatures related to mobile-immobile domain mass transfer processes (e.g., Singha et al., 2007; Swanson et al., 2012) and it has been successfully used to calibrate more refined solute transport models such as the Dual-Domain Mass Transfer (DDMT) model (e.g., Briggs et al., 2014; Day-Lewis et al., 2017).

The studies cited above demonstrate the potential of the DC method for studying solute transport and it has already been proven a most useful tool in numerous hydrogeologic studies. Nevertheless, several studies have highlighted serious limitations with common approaches to use DC resistivity data when aiming at obtaining quantitative information. A well-documented problem is the persistent under- and overestimation of mass and plume spreading, respectively, when relying on classical time-lapse ERI images (e.g., Singha and Gorelick, 2005; Laloy et al., 2012). These problems are to a large extent a consequence of ignoring that ERI images represent upscaled properties. As the data are noisy and incomplete, the ERI images are blurry smeared-out versions of the true electrical resistivity distribution. Some efforts have been made to develop more advanced data post-processing approaches (see, e.g., Singha et al. (2015) for a summary of approaches). At some point of the post-processing chain there is a need of using a petrophysical relationship to convert the upscaled electrical conductivity into pore-fluid conductivity (which is then easily converted into solute concentration (e.g., Sen and Goode, 1992)). Singha and Gorelick (2005) argue that it is the uncertainty surrounding this petrophysical relationship that is the main cause for the systematic failure mentioned above. This was demonstrated experimentally by Jougnot et al. (2018) using data representing large departures between the average tracer concentration predicted from measured apparent bulk electrical conductivity (translated into an average concentration by basic upscaling approaches) and the actual average concentration derived from the concentration distribution that was observed in their milli-fluidic laboratory experiment.

The most common and basic petrophysical relationship for transforming bulk electrical conductivity into fluid conductivity is Archie's law. It was first developed empirically (Archie, 1942) and later derived theoretically (Sen et al., 1981) using an Effective Medium Approximation (EMA) upscaling technique. This relationship assumes that the electrical conductivity of the pore water is constant in space and that measurements are made in an ergodic media (i.e., measurements are made over a representative elementary volume, REV). This is unlikely to be satisfied in the context of a tracer test. For example, if one considers a cross-section of the subsurface, gridded into 2-D squared elements, with a solute plume travelling across the medium from left to right, clearly, at the plume's front, where the tracer is progressively filling one of the 2-D square elements, the fluid conductivity (or tracer concentration) depends to a large extent on the position in the element. Furthermore, tracer heterogeneity varies on several scales, which implies that the square elements are likely to have sizes that are smaller than the REV scale. For both these reasons, Archie's law cannot be applied as is. This situation is depicted in Figure 2 that is modified from Jougnot et al. (2018). In Figures 2a and 2b, two screenshots of a steady-state flow field with a Heaviside tracer test injection are shown, where an electrically-conductive tracer progressively invades a square sample from left to right, while apparent bulk electrical conductivity samples are taken between two vertical line electrodes, represented by the vertical bold black lines at the left and right sides of the sample. In Figure 2c, the mean or apparent pore-fluid conductivity at the scale of the sample, S_w^{app} , inferred from the application of Archie's law to the measured apparent bulk electrical conductivity, S_b^{app} , is shown to increase non-linearly with time. This non-linearity offers a demonstration that the mean fluid conductivity inferred from Archie's law is biased. Such variations in the concentration distribution are expected not only when imaging plume boundaries, but also within the plume as the salinity distribution will vary at the pore scale and within small-scale unresolved geological heterogeneity.

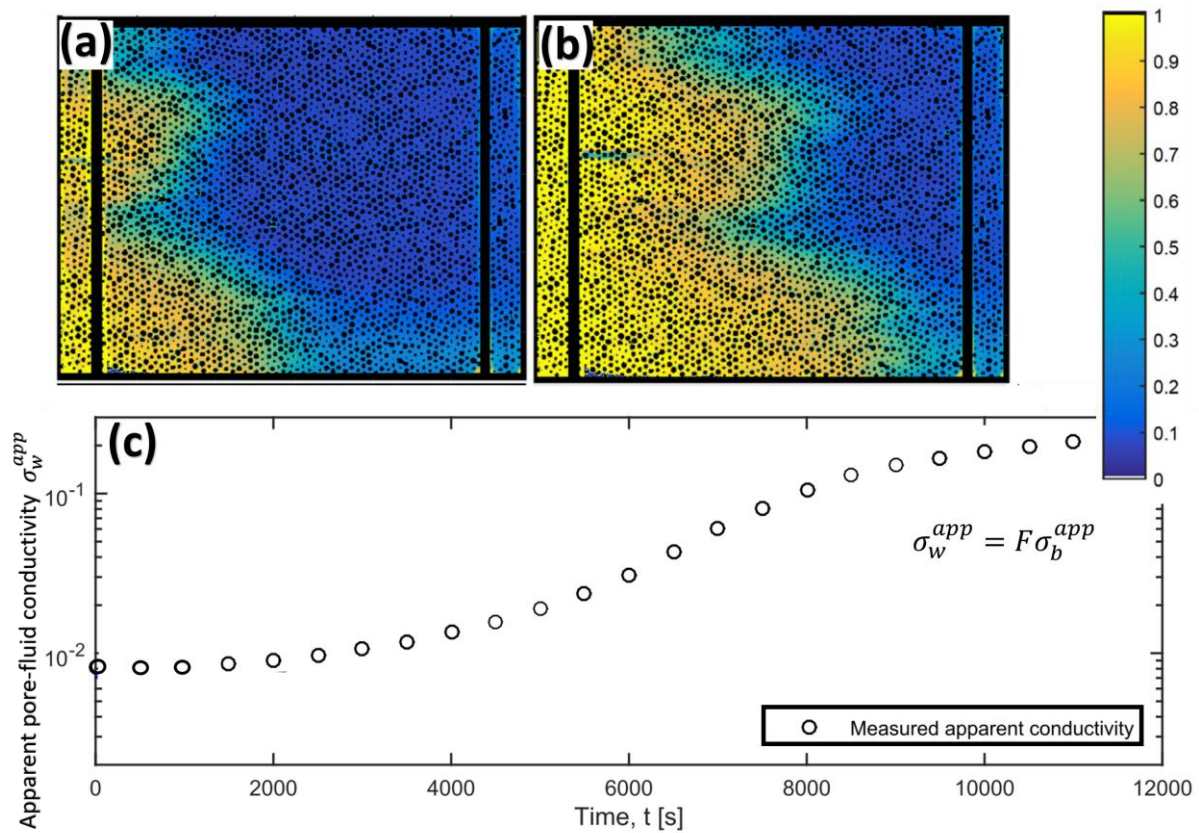


Figure 2: Milli-fluidic tracer test monitored with apparent bulk electrical conductivity measurements. (a) and (b) show two instances of the concentration field. (c) The time-evolution of the apparent pore-fluid conductivity, S_w^{app} , as predicted from the application of Archie's transformation (inset) to the measured bulk electrical conductivity at the scale of the sample, S_b^{app} , for a given formation factor F . The non-linear time-evolution of S_w^{app} for a steady-state flow field and Heaviside injection is testament to the failure of Archie's law to predict the average pore water conductivity. Modified from Jougnot et al. (2018).

The main research goal of ESR9 is to develop an upscaling framework relating the time-evolution of the non-stationary concentration fields for which no REV is defined with the corresponding time-evolution of the medium's apparent bulk electrical conductivity. More specifically, we seek to investigate to which extent time-series of apparent electrical conductivity parallel and perpendicular to tracer transport can constrain the mean concentration, its variance and connectivity measures of the concentration field. This is a challenging task and it is expected that the mapping will be non-unique, implying that only a probabilistic assessment about the statistical properties of the concentration field can be made. Using these advances, we expect to make inferences about the statistical properties about unresolved solute concentration heterogeneity and make statements about dominant transport regimes (e.g., ADE or DDMT). This will enable a more robust and enhanced approach to interpret DC resistivity time-series and offer the prospect of providing valuable information about in situ tracer properties that cannot be inferred from hydrogeological data alone.

Monitoring of biochemical reactions using spectral induced polarization

Various geophysical methods have been considered to constrain biochemical reactions (Binley et al. 2015). One suitable candidate method is spectral induced polarization (SIP). SIP provides information about the frequency-dependent complex electrical conductivity in the mHz to kHz frequency range (Kemna et al., 2012). The origins of the SIP signal include various factors such as porous media characteristics, aqueous phase saturation, microbial activity, and chemical reactions involving precipitation and redox reactions. Various laboratory studies have explored the possibility to monitor dynamic biochemical reactions in porous media using SIP measurements in biotic and abiotic conditions.

In abiotic conditions, previous studies have mainly focused on iron mineral and calcite precipitation. It was found that SIP measurements have a relatively high sensitivity to iron minerals. Several studies showed a strong relationship between the SIP response and the amount, specific surface area and transformation of iron minerals (Slater et al., 2005, 2006; Wu et al., 2005). Follow-up studies explored the possibility of detecting different processes associated with iron mineral, type of iron minerals and mineral size. For example, Ntarlagiannis et al. (2010) observed an increase in SIP response due to the secondary formation of iron sulfide precipitation in sand. Placencia-Gomez et al. (2013) found that oxidation of iron sulfide decreased the SIP response. The mechanism behind the strong polarization response of iron precipitation was clarified recently by Hubbard et al. (2014). In this study, it was confirmed that the polarization contribution of migration of charges within the magnetite particle dominates over the contribution from the electrical double layer. In the case of calcite precipitation, SIP is a potential geophysical method for in-situ monitoring in addition to the seismic method. However, knowledge about the SIP response of calcite precipitation is limited compared to the SIP response of iron minerals. Wu et al. (2010) were the first to report a clear SIP response of calcite precipitation in a laboratory study. Other studies reported much smaller and less clear SIP responses to calcite precipitation (Saneiyani et al., 2018; Zhang et al., 2012). More research is needed to clarify what environmental or mineral conditions determine the SIP response of calcite precipitation.

In biotic conditions, a range of studies investigated the SIP response associated with bacteria and biofilms. Ntarlagiannis et al. (2005) and Davis et al. (2006) cultivated bacteria and biofilms in column experiments and highlighted the possibility of applying SIP measurements to observe bacteria and biofilms. Abdel Aal et al. (2010) studied bioclogging and the associated change in hydraulic conductivity during cultivation, and suggested that the SIP response associated with biofilms is related mostly to clogging of pore throats. Zhang et al. (2014) measured the SIP response of bacterial suspensions with and without sand and obtained quantitative relationships between bacteria cell density and SIP response. They showed that the mechanistic model for SIP response of bacteria developed by Revil et al. (2012) cannot accurately reproduce the SIP response of bacteria in suspension. They also showed that the SIP response of bacteria in sand has a lower peak frequency than in suspension. Considering the dynamic habitat of bacteria in actual soils, further studies are necessary to obtain quantitative relationships between SIP response and properties of the microbial community, such as cell density, distribution in the measurement zone, activity and type of bacteria since all these properties possibly affect the chargeability of bacteria cells.

In addition to the SIP response directly associated with bacteria and biofilm, it has been shown that SIP has potential to detect mineral precipitation associated with microbial activity. Williams et al.

(2005) and Ntarlagiannis et al. (2005) were the first to report that the SIP response changed over time due to mineralization associated with microbial activity and bacterial growth (Zinc and Iron sulfide). Slater et al. (2007) used sulfate reducing bacteria to generate precipitation and subsequent dissolution of iron sulfide. They found that the SIP response increased with the amount of precipitation and decreased with dissolution of iron sulfide. They suggested that iron sulfide precipitation around sand grains was responsible for the observed SIP response. Wu et al. (2011) investigated the potential of monitoring calcite precipitation generated indirectly from bacteria activity in natural systems by using a sand column filled with sampled water from a field site. However, the SIP response in this study was weak and did not compare well with previous column experiments by Wu et al. (2010). Again, this suggests that further research is needed to simultaneously and continuously measure the SIP response and the relevant environmental conditions because the mineralization associated with microbial activity is dynamic in time and variable in space.

Some laboratory experiments have been conducted to replicate the bioremediation process aiming at a more direct application of SIP measurements. Abdel Aal et al. (2004) first reported that the SIP response can be affected by the microbial activity during biodegradation. Abdel Aal et al. (2006) and Mewafy et al. (2013) observed the SIP response of biodegradation and showed the potential to apply SIP measurement to monitor biodegradation. Recently, Noel et al. (2016) measured the SIP response, collected generated CO₂ gas and sampled water simultaneously during biodegradation of toluene. The SIP response of bioremediation has been also investigated in the field. The work on the Rifle Integrated Field Research Challenge (IFRC) site in the U.S. is a prime example. Flores Orozco et al. (2011) studied this site with SIP imaging, and suggested that mineral precipitation can be understood by combining SIP and chemical analysis. They also suggested that the SIP response is related to the activity of the Fe²⁺ ion. Additionally, they speculated that the effect of calcite precipitation is seen in SIP response. Based on the measured data, Chen et al. (2013) used a data-driven statistical model to obtain information about the biochemical stages of subsurface remediation. As shown above, bioremediation is one of the possible applications for SIP measurements. To our knowledge, however, quantitative information about in-situ biochemical reactions has not been obtained yet from SIP measurements.

As reviewed above, most SIP studies have been qualitative in nature because biochemical reactions are dynamic in both space and time and there are only limited ways to observe biochemical reaction in-situ in column setups for comparison purposes. Previous studies relied on indirect information such as sampling fluid and assuming that processes occur homogeneously in the measurement zone. This qualitative nature of previous laboratory setups has been a limiting factor for exploring the potential of SIP measurements to obtain quantitative information about dynamic biochemical reactions. The aim of the research by ESR12 is to quantify the relationship between biochemical reactions and SIP signals using a 2D cell containing a synthetic porous medium. This new measurement setup allows visualizing biochemical reactions while making SIP measurements. This will allow establishing more quantitative relationships between biochemical reactions and the SIP signal, and thus ultimately providing the opportunity to monitor biochemical reactions at the field scale in a more quantitative manner.

Full waveform ground-penetrating radar time-lapse imaging of tracer transport

Geophysical methods are increasingly being used in hydrogeological studies to characterize the structure and heterogeneity of the subsurface (Klotzsche et al., 2010) non-invasively to improve knowledge about flow and transport processes (Kemna et al., 2002; Singha and Gorelick, 2005). For instance, transport processes can be monitored using tracer experiments being monitored with crosshole ground penetrating radar (GPR) to derive temporal changes in electrical conductivity [σ] and permittivity [ϵ]. In recent years, crosshole GPR full-waveform inversion (FWI) have been shown to offer subsurface images with a decimeter-scale resolution between boreholes (Klotzsche et al., 2019a), and FWI tomograms co-located with well data were used to generate a deterministic adjoining planes facies model shown in Figure 3 (Gueting et al., 2017), which explained saline recent tracer test monitored by ERT (Müller et al., 2010).

An open question is to which extent crosshole GPR FWI time-lapse monitoring can be used to image transport processes. A numerical study imitating tracer tests in realistic conditions for an alluvial aquifer was performed to allow better prediction and planning of an optimized field tracer test. Four tracer types were considered, namely saline water, desalinated water, heat and ethanol with each having different physical properties (Seyfried and Grant, 2007; Glaser et al., 2012), and imaged by GPR FWI using different time-lapse inversion strategies (Asnaashari et al., 2015). The findings from the synthetic experiments were then tested in the field at the Krauthausen test site (Vereecken et al., 2000). An expected challenge in FWI of the field data is the time-varying physical properties at the boreholes due to tracer migration, which may affect the source wavelet (Klotzsche et al., 2019b). Improving field-scale resolution of transport processes will allow imaging preferential paths and often better-constrained plume imaging for use in hydrogeological models (Vanderborgh et al., 2005).

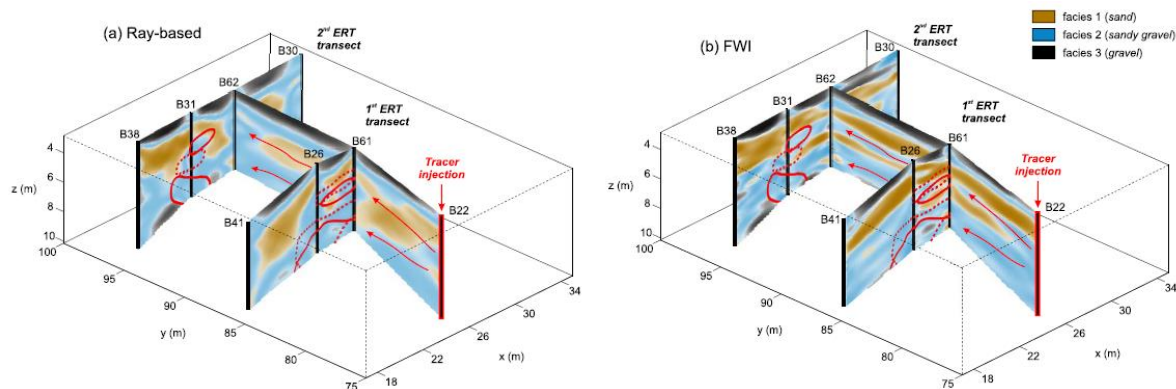


Figure 3: Comparison of ERT-inferred tracer transport paths and GPR predicted facies distribution using (a) dielectric permittivity obtained by ray-based inversion and (b) dielectric permittivity and electrical conductivity obtained by FWI. Red dashed and solid lines show the outlines of the ERT-inferred tracer plumes projected on the GPR tomograms. Facies model derived from FWI could explain the plume splitting, which the ray-based inversion could not (adopted from Gueting et al., 2017).

Innovative tracers to image subsurface processes

Tracers are very useful for imaging subsurface dynamics and deriving important transport information needed to parameterize groundwater models (Maliva, 2016). The choice of tracer type depends mainly on the aquifer system being studied and the investigation purpose (Maliva, 2016; Ptak et al., 2004). Saline and dye tracers are useful to infer fast advective transfer (preferential pathways), but are of limited value for quantifying matrix processes (Bodin et al., 2003; Domenico and Schwartz, 1998; Tsang and Neretnieks, 1998). Several tracer test interpretations confirm that diffusion is a matrix process that needs to be considered (Bodin et al., 2003; Maloszewski and Zuber, 1993; Meigs and Beauheim, 2001; Neretnieks et al., 1982; Reimus et al., 2003). This is particularly true when double porosity effects such as matrix diffusion or immobile water are important. In such settings, solving only the ADE offers limited predictive capabilities (e.g. Bodin et al., 2003). Thus, new innovative tracers such as dissolved gas or heat are needed to provide cost-efficient means to derive information about matrix processes or immobile water (Anderson, 2005; Chatton et al., 2017; Kurylyk and Irvine, 2019). Clearly, advanced and more complete modeling approaches can only be used effectively if there are data available to constrain additional processes.

Robust and reliable transport predictions are best met when using a model informed by tracer information together with a realistic assessment of aquifer structures and occurring processes. For this reason, one goal of ESR11 is to advance the interpretation of artificial dissolved gas injections and natural or artificially-caused temperature signals.

Dissolved gases such as Helium, Argon and Xenon are inert and have higher diffusion coefficients than solutes (e.g. Helium (10°C): $5.88 \cdot 10^{-9} \text{ m}^2 \text{ s}^{-1}$; Jähne et al., 1987). Since mass spectrometers are increasingly mobile and portable (Brennwald et al., 2016) and allow for site-continuous measurements (Chatton et al., 2017), artificial dissolved gas injections are one innovative new approach to image the variation of diffusion processes with distance from the injection well and to overcome restrictive modeling assumptions that neglect diffusion. With this in mind, ESR 11 performed in 2018 a dissolved gas injection using the continuous flow membrane inlet mass spectrometer (CF-MIMS) by Chatton et al. (2017) within a high-porosity chalk aquifer.

Temperature differences offer a second promising tracing possibility, but is only rarely used and can be considered underutilized for aquifer characterization (Kurylyk and Irvine, 2019). For example, hot water injection (i.e., injection with water temperatures above groundwater temperature) can be used to image heat transport behavior. In comparison to a salt or a dye tracer, heat (diffusion coefficient around $10^{-6} \text{ m}^2 \text{ s}^{-1}$) behaves non-conservatively as there is a loss to the matrix, thereby, retarding the transport (Anderson, 2005). Compared to a reactive tracer, less chemical process understanding (e.g. isotherms) is required. Thus, for local-scale investigations, heat is a most suitable tracer to image matrix processes and dynamic changes of fluid properties such as density and viscosity (Anderson, 2005; Irvine et al., 2015). Recent examples involving hot water injections are given by Wildemeersch et al. (2014) in a porous alluvial aquifer in Belgium, by Sarris et al. (2018) in porous sandy gravel with occasional sand and open framework gravel lenses at the Burnham experimental site in New Zealand and by Read et al. (2013) in a fractured granite in France. Within ENIGMA, ESR11 used the data from Wildemeersch et al. (2014) for stochastic modelling (Hoffmann et al. 2019) and applied a hot water injection in a high porosity chalk, which is a complex double porosity media and a different aquifer type than those considered in previous studies.

If the natural aquifer background temperature is high, for example, around 30°C in India (Groundwater temperatures worldwide: Benz et al. (2017)), the usefulness of injecting hot water is questionable. For this reason, ESR 11 relied on cold-water injection (i.e. the injection water temperature is below the groundwater temperature). In such a system, the use of cold water allows studying the heat released from the matrix to the colder circulating fluid and offers a suitable alternative to hot water injections for studying how density and viscosity impacts transport.

Both hot and cold-water injections cause reversible temporary changes in the aquifer that can be imaged by geophysics. This can be used to achieve time-lapse observations in the subsurface that ultimately make groundwater models more precise and reliable. Nevertheless, when combined tracer experiments are used (e.g. joint heat-solute injections), then more complex groundwater models are required. For instance, the choice of the right fracture geometry is a challenge as recent analytical solutions show that heat transport seems to prefer a channel geometry while a solute tracer seems to prefer a plane structure (e.g. de La Bernardie et al. (2018)). For ESR11, unique parameterizations are to be questioned and should rather be replaced by data science tools (e.g. Monte Carlo simulation within the Bayesian Evidential Learning framework presented by Hermans (2017)).

Achieved and on-going activities, results and challenges

In this section, we describe the achieved and ongoing research activities. Particularly, we focus on the experiments that have been carried out, the results obtained and the various challenges that are still to be resolved.

Electrical signatures of spreading and mixing: Towards an upscaling framework

ESR9 is currently developing the various puzzle pieces needed to build an upscaling framework. First, ESR9 performed a laboratory experiment to investigate the signature of saline diffusion on apparent electrical conductivity in a 2-D medium. In this work, a fluorescent and electrically conductive tracer is injected in a Hele-Shaw cell, confining an artificial (2-D) porous medium, which consists of 0.4 mm-thick cylindrical silicon (polydimethylsiloxane, PDMS) pillars. The setup and the following description refer to Figure 4. The fluorescent tracer is excited with a light source placed above the cell, and the light emitted from the sample is recorded over time with a camera placed below, which allows monitoring how the 2D field of tracer concentration evolves over time. Concurrently, electrical current is injected in two alternating modes, horizontally and transversally, from the two pairs of Injection electrodes $A_H - B_H$ and $A_T - B_T$, respectively. The apparent resistivity is monitored using 12 potential electrodes for each of the injection modes controlled with a computer interface.

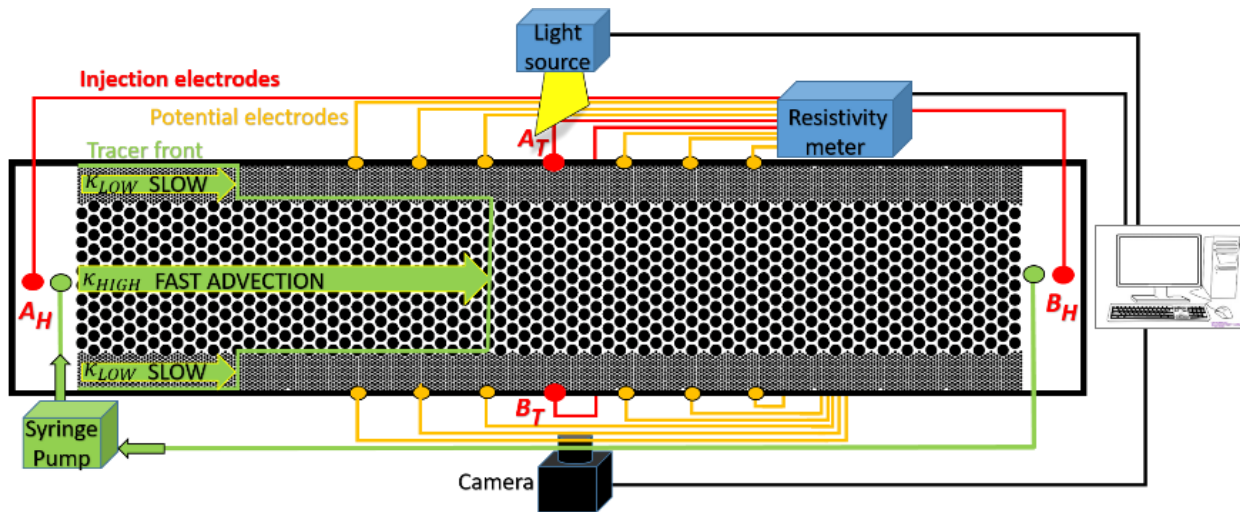


Figure 4: Experimental setup of an artificial 2-D layered porous medium within which a tracer test is executed with a syringe pump. The cell is equipped with fluorimetric (light source and camera) and geophysical (potential electrodes, injection electrodes and resistivity meter) monitoring capabilities. The computer represented on the right side coordinates all the measurement operations.

With this layered design, the electrical signature of the conductive tracer invading the medium is separated in time in two parts: first, the “advective” signal, caused by rapid horizontal invasion along the high permeability channel ($\kappa_{HIGH} = 16\kappa_{LOW}$) and, second, after the injection has been stopped, the “diffusive” signal, caused by slow, transversal invasion through diffusion.

The processing and interpretation of the tracer test experiments are currently ongoing. We are also currently focusing on a numerical study for assessing the amount of information contained in such electrical conductivity time-series with respect to the underlying hydraulic conductivity field controlling the flow field, which ultimately controls to a high degree, the solute transport regime and, thus, the time-evolution of the concentration field heterogeneity that we aim to constrain.

For performing such analysis, we work with synthetic ionic tracer tests executed in a 2-D squared domain of unit length, which is electrically monitored by measuring horizontal and vertical apparent electrical conductivity time-series. The numerical experimental setup is similar to the one shown in Figure 4, but with the addition of line electrodes in the top and bottom boundaries. The tracer tests consists of a steady-state flow field, established by imposing a constant pressure gradient between the vertical faces of the domain (such that the sense of mean flow direction is from left to right) with a continuous injection from the left side of the domain of a fluid with an electrical conductivity that is 100 times higher than the conductivity of the in-situ solution. While the conductive tracer is invading the domain, samples of horizontal and vertical equivalent electrical conductivity are obtained, respectively, by alternatively applying a voltage difference between the vertical and horizontal electrodes, respectively, and by calculating the subsequent electrical current flowing through the sample for each case.

The reason for using this setup is two-fold. First, it can be well reproduced in the laboratory implying that our conclusions can be easily transferred to such studies. Second, from a theoretical point of view, this setup is designed to assess the fundamental properties of equivalent (apparent) conductivity time-series. This latter feature is very important to better understand how to construct the upscaling framework.

Synthetic tracer tests are performed in different multi-Gaussian hydraulic conductivity fields (e.g., Rubin, 2003) that differ in their type of heterogeneity, represented by their variance and their structure quantified by their covariance (e.g., Delfiner and Chilès, 1999). The objective of the study is then to assess the ability of using the equivalent electrical conductivity time-series to infer the geostatistical model parameters. We approach this problem through a formal Bayesian inference framework (e.g., Gregory, 2005).

Figures 5 and 6 illustrate how the effective electrical conductivity time-series differ in response to the degree of hydraulic heterogeneity. Figures 5a and 5b, respectively, represent a screenshot of the time-evolving concentration field and the electrical and mass breakthrough curves for a tracer test performed in a hydraulic conductivity field with a low level of heterogeneity. The advecting tracer produce an almost planar front and the horizontal and vertical equivalent conductivities evolve largely following the well-known analytical upscaling formulas for this laminated case, which are the harmonic and arithmetic means, respectively. In Figures 5c and 5d, the time-derivatives of the equivalent horizontal and vertical conductivities are compared with the time-derivative of the mass breakthrough curve. The time-derivative of the horizontal electrical conductivity is highly sensitive to the first tracer arrival and shows correlation with the derivative of the mass breakthrough curve (Figure 5c), whereas the time-derivative of the vertical conductivity remains approximately constant for the whole experiment, showing a linear (arithmetic) scaling with time as the tracer fills the medium from left to right.

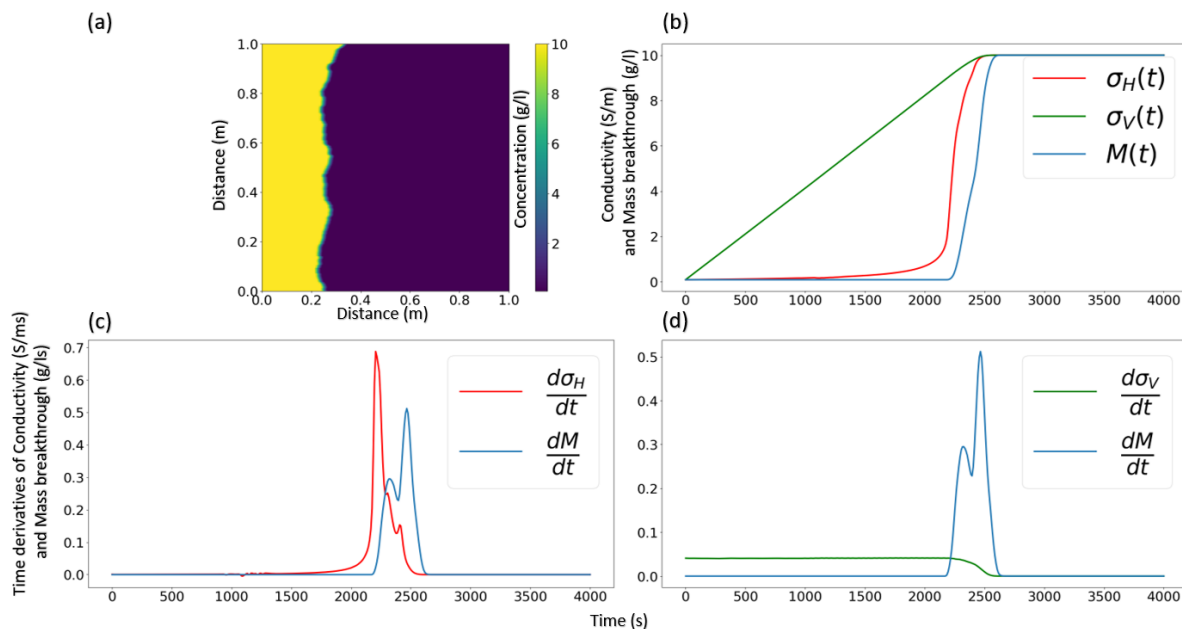


Figure 5: Electrical and mass breakthrough curves for a tracer test in a hydraulic conductivity field with a low level of heterogeneity. (a) Screenshot of the concentration field at the middle of the tracer test at time 500 s, (b) time-series of horizontal (red line) and vertical (green line) equivalent conductivity and the mass at the outlet (blue line). (c) Time-derivative of horizontal conductivity (red line) and mass breakthrough curve (blue line). (d) Time-derivative of vertical conductivity (green line) and mass breakthrough curve (blue line).

In Figures 6a and 6b, respectively, a screenshot of the time-evolving concentration field and the electrical and mass breakthrough curves are shown for the case of a much more heterogeneous hydraulic conductivity field. In Figure 6c it can be seen that the time-derivatives of the equivalent horizontal conductivity and mass breakthrough curves have similar shapes and are much more dispersed over time due to the wide variability of tracer arrival times. The vertical conductivity increases in a slower manner than the less heterogeneous case as connected conductive connected tracer paths in the vertical direction are rare.

The results from the laboratory tests, together with the results from the numerical study constitute a first step towards the construction of a framework that will enhance our ability to exploit conductivity time-series for recovering valuable information regarding the underlying solute transport regime. Specifically, the numerical study has resulted in a database of 100'000 time-series of concentration fields with their corresponding electrical conductivity time-series. This wealth of information is currently analyzed to decipher connections between the time-evolution of statistical and morphological descriptors of the concentration field and the time-evolution of the equivalent electrical conductivity.

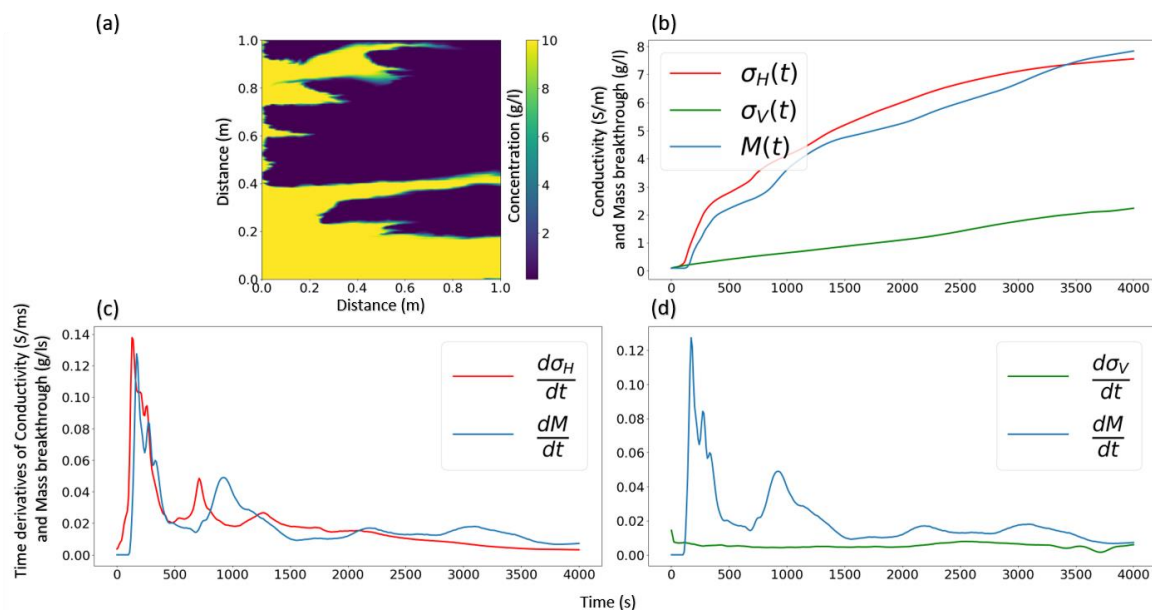


Figure 6: Electrical and mass breakthrough curves for a tracer test in a hydraulic conductivity field with a high level of heterogeneity. (a) Screenshot of the concentration field at the middle of the tracer test at time 500 s. (b) Time-series of horizontal (red line), vertical (green line) equivalent conductivity and the mass at the outlet (blue line). (c) Time-derivative of horizontal conductivity (red line) and mass breakthrough curve (blue line). (d) Time-derivative of vertical conductivity (green line) and mass breakthrough curve (blue line).

Monitoring of biochemical reactions with spectral induced polarization

Calcite precipitation was chosen to assess the ability of monitoring biochemical reactions with SIP. First, the effect of solute composition on the SIP response of calcite precipitation was investigated using a sand column experiment. The results showed that the SIP response of calcite is highly

sensitive to the solute concentration near the precipitates, which may explain previously reported conflicting results (Izumoto et al., 2019). Next, the 2D cell with a synthetic porous media (Height: 1 mm, Porosity: 0.59, Average pore throat: 0.41 mm) with electrodes for SIP measurement was developed (Figure 7). The SIP signal was measured with different pairs of potential electrodes 1, 2, 3 and 4. In combination with a normal camera and high-zoomed camera, the development of calcite precipitation was visually monitored at global (Figure 8) and local (Figure 9) scales while measuring the SIP signal. The high-zoomed camera was incorporated with a 2-axis moving table so that the whole measurement area (5 cm × 10 cm) can be monitored with a resolution of 1 $\mu\text{m}/\text{pixel}$ during the experiment. After the experiments, the porous media was taken from the setup for further analysis of the calcite precipitation. Importantly, we succeeded in duplicating the SIP signals in two experiments showing that the SIP responses (Figure 10) and the patterns of calcite precipitation (Figure 8) are reproducible. Post processing of the obtained images and analysis of calcite precipitation is ongoing. In addition, the simulation of reactive transport and SIP responses at the pore scale using the open source FVM software OpenFOAM and the measurements of SIP responses of growing microbes (*Shewanella*) are on-going.

Sample holder + 2D porous media

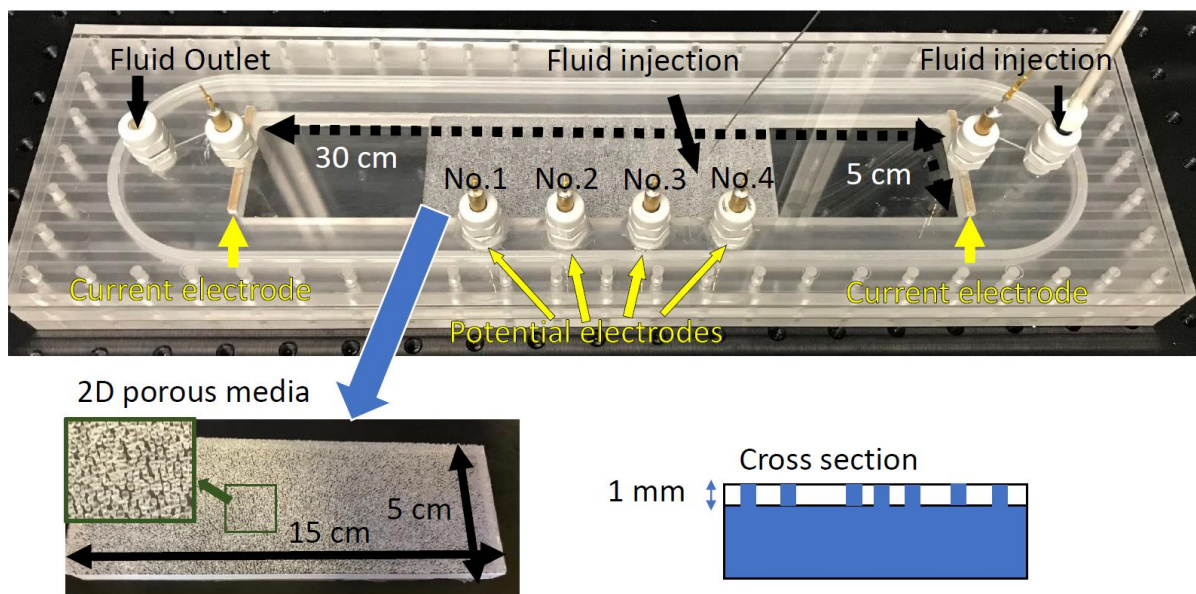


Figure 7: 2D cell with a synthetic porous media (height: 1 mm, porosity: 0.59, average pore throat: 0.41 mm) with electrodes for SIP measurements.

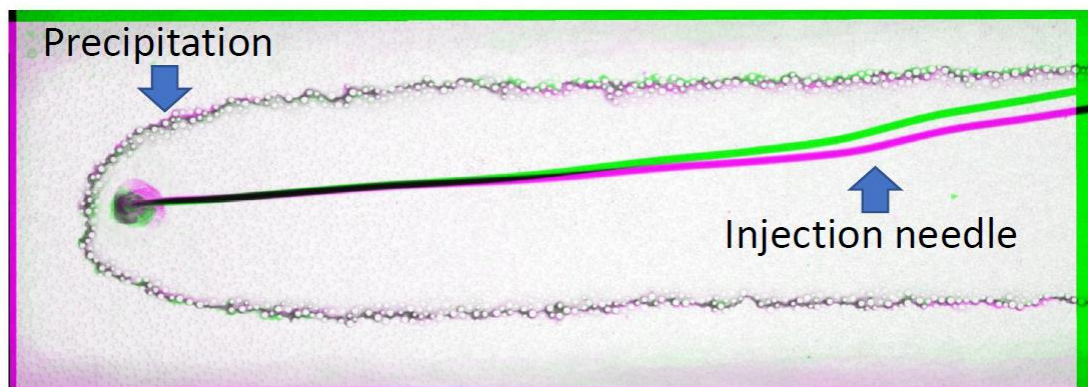


Figure 8: Calcite precipitations in the porous media at the end of the experiments. Different colors are used to represent the results of the two repeat experiments.

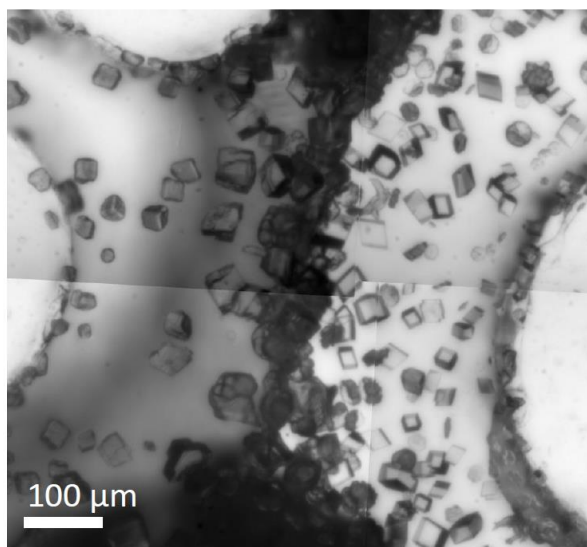


Figure 9: Example of an image taken by the high-zoomed camera with the rhombohedron crystals being calcite precipitates.

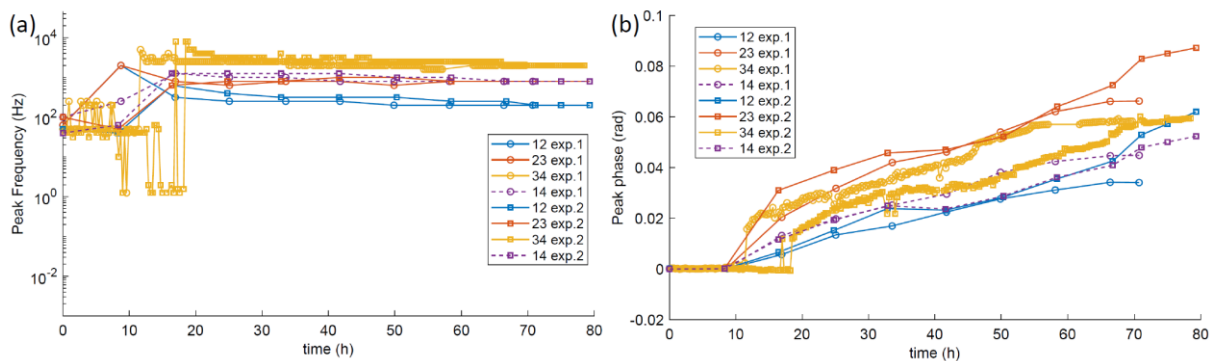


Figure 10: (a) Peak frequencies and (b) peak phases over time for different electrode pairs (1-2, 2-3, 3-4 and 1-4) in the repeat experiments (exp.1 and exp.2).

Full waveform ground-penetrating radar time-lapse imaging of tracer transport

Within the project of ESR10, we applied GPR FWI to characterize flow and transport processes within a gravel-sand aquifer using different tracer types. The aim is to investigate the ability of crosshole GPR FWI to monitor and map different types of tracer plumes during time-lapse experiments. To guarantee successful performance of the different planned tracer experiments, we started by conducting a synthetic study to optimize the acquisition, processing and inversion strategies.

To establish this numerical study, we first developed a realistic high-resolution aquifer model of the Krauthausen test site based on the large amount of available data at this site. This model was generated using stochastic geostatistical realizations of hydrologic properties (hydraulic conductivity and porosity) and GPR parameters (dielectric permittivity and electrical conductivity) considering their vertical and horizontal correlation lengths. Solute transport simulations were used to simulate tracer experiments and synthetic time-lapse (TL) GPR data were generated using finite-difference time-domain modeling at several time instances after the tracer injection. Different synthetic tracer tests were investigated to assess the tracer type with the largest impact on the permittivity or electrical conductivity images resulting from the FWI. One of the main purposes of this numerical study of time-lapse crosshole GPR FWI was to investigate how accurate the tracer plumes can be detected and to develop approaches to optimize plume reconstruction.

We performed the FWI for the background (BKGD, no tracer applied to the aquifer) GPR data set and at different time steps after tracer injections. We also investigated different inversion strategies and starting model options to enable a stable, fast, and reliable FWI at the different time steps. To visualize the tracer plume, the FWI results are subtracted from the background FWI results. Important questions that were addressed with these synthetic tests are: (i) how much tracer is needed to ensure detection by the FWI and (ii) what is the optimal borehole setup and acquisition strategy. The results of these synthetic tests will be used for designing upcoming field experiments at the Krauthausen site where the different tracer types will be applied to enhance our understanding of the Krauthausen aquifer and the ability of FWI GPR to constrain transport processes. The two tested inversion strategies used to assess the physical parameter changes are 1) separate FWI inversions (M1) and 2) inversion of the difference data with respect to the reference data (M2). For both strategies, different starting model (SM) options were investigated using either a smoothed model of the real reference model (RM) or final results of the background FWI results ((i) ϵ and σ

from smoothed RM; (ii) ϵ from BKGD FWI and σ from smoothed RM; (iii) ϵ from smoothed RM and σ from BKGD FWI; and (iv) ϵ and σ from BKGD FWI).

For a saline tracer (σ changes only), the numerical test demonstrates that the M2 method using as SM the recovered BKGD ϵ and σ models provided the most accurate result (Figure 11), compared to M1, which produces TL artifacts at locations where the plume is not present. This is probably caused by the fact that unexplained data events (non-fitted during inversion) stay common for both the baseline and monitoring data when using M2 and will therefore not cause TL artifacts. Reconstruction of the plume shape and σ TL changes is successful down to a ~ 0.2 m scale, however preferential flow paths with thicknesses on the order of 0.1 m are smoothed out compared to the real plume. For a tracer causing both ϵ and σ changes (e.g., ethanol tracer), the plume could be reconstructed from both ϵ and σ changes (Figure 12), where ϵ changes provided the best reconstruction.

The findings of the numerical study were tested in two field-scale tracer tests that were monitored by crosshole GPR. In the first tracer experiment, a positive saline tracer (positive change in σ) and in the second test water with a higher temperature compared to the ambient temperature (positive change in σ , small negative change in ϵ) was injected into the aquifer. In total, we measured 80 GPR planes and the experimental data are currently being analyzed and inverted. From observation of GPR data, clear time-lapse changes of attenuation and arrival times are seen that are consistent with the tracer data monitored with borehole loggers.

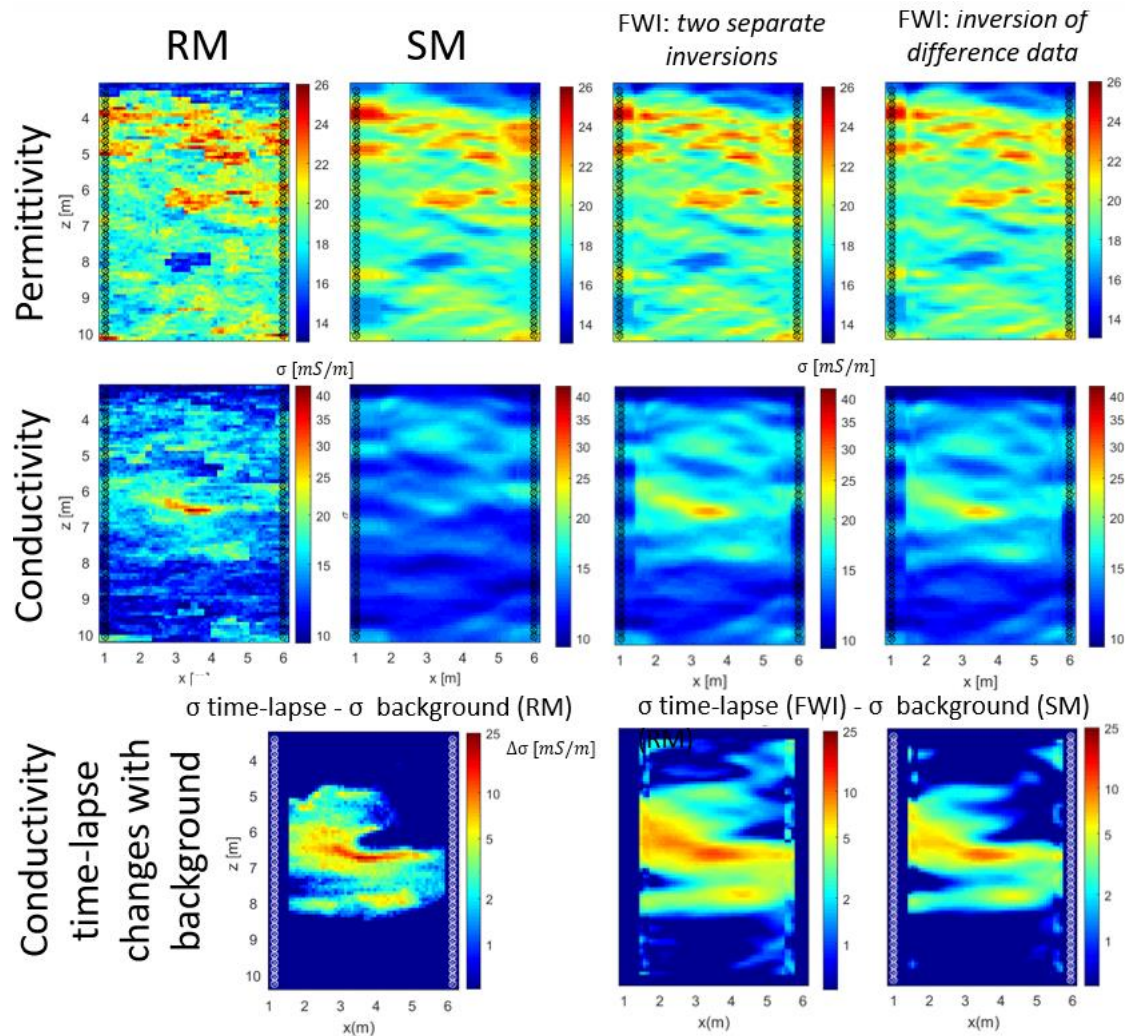


Figure 11: Plume reconstruction of salt tracer (electrical conductivity changes only). Results of two FWI methods are compared to the true model (bottom row) show that inversion of difference data (right) provides a better plume reconstruction.

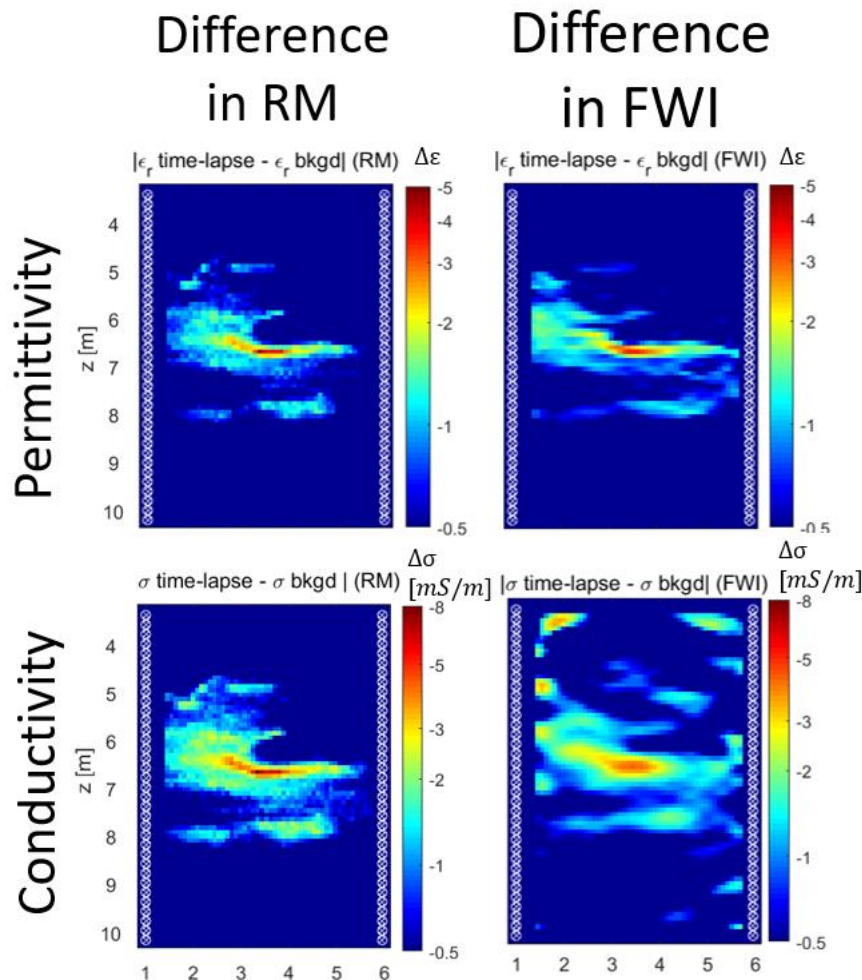


Figure 12: Plume reconstruction for ethanol tracer (causing negative changes in both permittivity and electrical conductivity) using two separate inversion method where time-lapse SM was based on time-lapse dataset. Changes in permittivity provide better reconstruction than electrical conductivity.

Innovative tracers to image subsurface processes

The main focus of ESR11 is multi-scale characterization of transport in heterogeneous porous and fractured media aquifers. A major emphasis is placed on using innovative heat and solute tracer test data for detecting preferential flow and transport paths and to assess their value in the context of transport modeling. A reached milestone is the publication of a first paper in the open access journal "Frontiers in Earth Science" (Hoffmann et al., 2019). This paper deals with innovative numerical modeling of a pre-existing joint heat and solute tracer test data acquired in alluvial sediments by Wildemeersch et al. (2014). Numerical simulations using a Monte-Carlo approach allow for prior uncertainty quantification and a distance-based sensitivity analysis (i.e. steps 1 to 4 in the Bayesian Evidential Learning (BEL) procedure presented by Hermans (2017). During the prior uncertainty investigation, prior realizations with different parameterization may reproduce the data at each of the 19 temperature observation points. This highlights the importance of a realistic spatial parameter distribution. Further, compared to solute transport, it seems that models considering less heterogeneity represent the heat distribution better. This implies that conduction is important to consider and that a significant part of the pore space might be occupied by immobile water.

In comparison with local sensitivity analysis, the performed distance-based sensitivity analysis better quantifies the relationship between input and model response uncertainty. Thus, it reveals useful information about the parameters that most influence the model outcomes. For example, if heterogeneity is represented realistically by an increasing K-trend distribution with depth respecting the borehole geometry, then heat transport seems less sensitive to advective parameters (e.g. porosity) compared to solute transport. This is consistent because (a) heat and solute tracer have a complementary nature and (b) the test site Hermalle-sous-Argenteau is a strongly advective system, where the solute tracer is more influenced by advection in comparison to the heat, for which the effect of conduction remains important to consider for transport modelling. Thus, the study shows, that spatial heterogeneity has a major influence on the simulation results and heat transport interpretation gives added aquifer system information.

By comparing both types of tracer velocities, the non-falsified prior realizations (i.e., those that are not rejected in the Monte Carlo simulations) describe the observed joint heat and solute tracer behavior better than previous deterministic solutions. This implies that this test site can be described in a more realistic manner when using stochastic models (Monte-Carlo) compared with previously proposed deterministic approximations. Such considerations are important for any kind of application demanding robust transport process.

The performed injection tests with hot water and artificial dissolved gas, jointly injected with a dye tracer in a chalk aquifer in Belgium, using a convergent flow field gave new and useful field data to support ongoing fractured rock groundwater flow and transport modeling. So far, the main results consist in local fracture geometry information (e.g. deduced from analytical solutions) and matrix diffusion information. The results clearly highlight the difference between the advection-dominated transport of solute and the complementary behavior of the heat transport. Clearly, the two tracers are affected differently by the double porosity nature of the chalk.

Another field data set has been acquired using multiple hot and cold water injections in a weathered granite system in South India. Future simulations of these experiments promise to offer a reliable assessment of the main transport parameters, an estimation of the rock matrix porosity, and a quantification of the effect on transport by viscosity changes caused by hot and cold water injections. Thanks to the injection of hot and cold water, processes like storage and delivery of heat energy, can be studied and compared for the same matrix. Once the main transport parameters have been constrained, a temperature-dependent sensitivity analysis will follow. In connection with the quantification of the viscosity changes, the influence on heat transport can be assessed.

The numerical reproduction of all field data is challenging, but also very promising to understand how heat and cold water tracer tests add hydrogeological information. To our knowledge, cold water was here used for the first time as an artificial tracer. Could we expect a different behavior than hot water due to differences in viscosity and buoyancy? The detailed interpretation that is currently ongoing will answer this question.



Link between data and models

During the electrically monitored tracer test, ESR9 obtained photographs from the evolving 2-D concentration field and also time-series of electrical conductivity measured at different locations within the porous cell. Given the design of the experiment, this data set consists of simultaneous observations of tracer diffusion and the time evolution of bulk electrical conductivity of the cell, something that will enable us to directly relate the former with the latter for prediction purposes.

ESR12 obtained images of calcite precipitation and associated spectral induced polarisation signals during laboratory experiments. Based on destructive analysis that is planned after the experiments, the height and weight of the precipitation will be measured. These data will provide information about the mass, distribution and grain size of the precipitation over time. They can support the establishment of quantitative relationships between the SIP response and calcite precipitation process, thereby, advancing fundamental modeling understanding about SIP signals and their use in the context of monitoring reactive transport processes such as calcite precipitation at the field scale.

For ESR10, the data and FWI strategies used may provide improved plume reconstruction based on temporal changes in GPR data and inferred parameters. In a solute transport context (e.g., salt tracer monitoring), the improved resolution offered by this combined approach enable determination of the thicknesses of preferential transport paths. Appropriately converting the geophysical parameters to solute concentrations can provide detailed input for groundwater modeling that can be used to enhance the modeling capabilities compared with conventional methods. Using a heat tracer where the plume is partly transported by conduction through the solid material, it is anticipated that spatial imaging of mobile and immobile water regions through variations in heat capacity and thermal conductivity may be possible. This information may be useful for enhanced understanding of heat storage and to improve modeling approaches.

Robust transport predictions using numerical groundwater models require a realistic conceptualization of subsurface heterogeneity. It is also necessary that simulated data responses agree well with sampled observational data. At the first test site (Hermalle-sous-Argenteau) considered by ESR11, he used previously published data in his first publication (Hoffmann et al., 2019). At the sites in Mons and India, ESR 11 collected his own joint heat and solute tracer data to support ongoing modeling efforts. Thanks to the complementary nature of these tracers, both the velocity variance (derived from the solute tracer) and the mean velocity (derived from the heat tracer) can be used for modeling purposes. This allowed a simultaneous interpretation of structures (e.g., pathways) and processes (e.g., matrix diffusion linked to heat conduction). This is one possible way to constrain diffusion processes in ground water models for more realistic heterogeneity characterization. In this context, data science tools (e.g. direct predictive approaches like Bayesian Evidential Learning) appear promising for improved groundwater management.

Added-value of the network

The network provides the ESRs with two great opportunities: first, working as a team with other ESR students in topics that are closely related to their PhD projects, which can be very stimulating, and, second, being in contact with world-leading experts in a myriad of related topics. For instance, ESR9 had the opportunity of being in contact with geophysics experts (UNIL) and solute transport experts

(CNRS Rennes and CSIC), coming both from theoretical and experimental communities. It is virtually impossible to find one academic supervisor that possesses all these skills.

The project of ESR12 is running in collaboration between FZ Jülich (main host) and CNRS Rennes (secondment). Development of the measurement system, analysis of the obtained data and simulations have been achieved in close collaboration. The cell with SIP electrodes used to contain 2D porous media was developed at FZ Jülich, while the porous media, normal camera, 2-axis table and high-zoomed camera were prepared at CNRS Rennes. They have recently been assembled at CNRS Rennes. As for data analysis, the obtained SIP responses and the simulation of SIP response are discussed mostly at FZ Jülich. Image analysis and simulation of reactive transport are made at CNRS Rennes. These analyses will be used for quantification of SIP responses of calcite precipitation processes and further for simulating SIP responses and calcite precipitation processes. This implies that technical experimental skills related to laboratory experiments are shared among the partners and that complimentary expertise in SIP and reactive transport are effectively combined.

For the GPR-monitored saline tracer test operated by ESR10, AQUALE Enigma partner provided borehole electrical conductivity loggers. For the GPR-monitored heat tracer test organized by ESR10, ESR6 provided borehole temperature loggers and ESR11 provided and managed the heat pump equipment to enable successful GPR monitoring of a heat tracer (i.e. hot water injection with a temperature difference of around +30 °C) experiment. This is an example of how the network enables the combination of innovative process-based transport imaging techniques (i.e. heat tracing) with the most innovative GPR tools (i.e. full waveform inversion) in order to achieve the highest possible resolution from geophysical imaging of transport processes. The frequent project meetings and workshops within ENIGMA and the secondments are effective tools to initiate and pursue such common experiments and collaborations. For instance, the involvement of ESR11 in the above-mentioned field experiment was facilitated by his three-month secondment (May 6 until August 06 2019) at FZ Jülich

For ESR11, the six-month secondment at BRGM (French Geological Survey) in both India and France provided a firsthand experience of applied science (this secondment will finish in November 2019). During the fieldwork in India, additional worthwhile experience abroad was achieved with a positive impact on the ESR's personal development and his scientific career perspectives. Thanks to the network, knowledge transfer from theory to practice and a fruitful cultural exchange was achieved.

Dissemination activities

Fernandez, A., de Anna, P., Jougnot D., Méheust Y., Le Borgne T., & Linde N. (2018) Millifluidic tracer experiments to investigate the signature of saline diffusion on effective electrical conductivity. 4th Cargèse Summer School: Flow and Transport in porous and fractured media. Cargèse (Corsica, France) (poster)

Haruzi, P., Gueting, N., Klotzsche, A., Vanderborght, J., Vereecken, H. and van der Kruk, J. (2018). Time-lapse ground-penetrating radar full-waveform inversion to detect tracer plumes: A numerical study. In SEG Technical Program Expanded Abstracts 2018 (pp. 2486-2490). Society of Exploration Geophysicists

- Haruzi, P., Zhou. Z., Klotzsche, A., Vanderborght, J., Vereecken, H. and van der Kruk, J. (2019) High resolution characterization of time-lapse tracer experiments using crosshole GPR full-waveform inversion: A synthetic study. The 6th International Conference "Novel Methods for Subsurface Characterization and Monitoring: From Theory to Practice". University of Waterloo, Canada (oral)
- Hoffmann, R., T. Hermans, P. Goderniaux and A. Dassargues (2018) Prior uncertainty investigation of density-viscosity dependent joint transport of heat and solute in alluvial sediments. Computational Methods in Water Ressources XXII - CMWR 2018. Saint Malo (France) (oral)
- Hoffmann, R., P. Goderniaux, and A. Dassargues (2018) Multi scale transport modelling in heterogenous porous and fractured media. 4th Cargèse Summer School: Flow and Transport in porous and fractured media. Cargèse (Corsica, France) (poster)
- Hoffmann, R., P. Goderniaux, A. Poulain and A. Dassargues (2018) Fractured aquifer heterogeneity characterization for advanced transport modelling based on multiple single fracture tracer tests. 45th IAH Congress - Groundwater and Life: Science and Technology into Action. Daejeon (South-Korea) (oral)
- Hoffmann, R., P. Goderniaux, P. Jamin, and A. Dassargues (2018) The double porosity of the chalk and its influence on solute and heat transport. 6th International Geologica Belgica Meeting 2018. Geology Serving Society. Leuven (Belgium) (oral)
- Hoffmann, R., A. Dassargues, P. Goderniaux, and T. Hermans (2019). Heterogeneity and prior uncertainty investigation using a joint heat and solute tracer experiment in alluvial sediments. *Frontiers in Earth Science – Hydrosphere*: **7** (108). doi: 10.3389/feart.2019.00108
- Hoffmann, R. (2019) Cold water injections in South India – An innovative smart tracer technique for hot fractured aquifers. H+ Network meeting 2019. Paris (France) (invited talk)
- Hoffmann, R. (2019) Process-based imaging using as innovative smart tracer dissolved gas, heat and cold water. IBG-3 Seminar at FZ Jülich. Jülich (Germany) (invited talk)
- Hoffmann, R., P. Goderniaux, and A. Dassargues (2019) Transport heterogeneity quantification in heterogeneous fractured media-Chalk. Journée du département de l'UR ArGEnCo/UEE. Department of Urban and Environmental Engineering-Liege University (poster)
- Hoffmann, R., P. Goderniaux, and A. Dassargues (2019) Dissolved Gas, Heat and Cold water as innovative smart tracers for transport heterogeneity characterisation in fractured media. 10th International Groundwater Quality Conference. Liege (Belgium) (oral)
- Hoffmann, R., A. Dassargues, P. Goderniaux and T. Hermans (2019) Modeling a heat tracer test in alluvial sediments using Monte-Carlo: On the importance of the prior. 46th IAH Congress – Groundwater management and governance coping with water scarcity. Malaga (Spain) (poster)
- Hoffmann, R., W. Uddin, P. Goderniaux, A. Dassargues, J.-C. Maréchal, S. Chandra, V. Tiwari and A. Selles (2019) Cold water injections as innovative smart tracer technique in hot fractured aquifers. 46th IAH Congress – Groundwater management and governance coping with water scarcity. Malaga (Spain) (poster)
- Hoffmann, R., P. Goderniaux, and A. Dassargues (2019) The potential of temperature and dissolved gas as smart tracers for process-based heterogeneity characterization. American Geophysical Union Fall Meeting. San Francisco (C.A.) (will be given as oral)

Izumoto, S., J. A. Huisman, E. Zimmermann, O. Esser and F.-H. Haegel, H. (2018) Spectral induced polarization response of calcite precipitation. 5th International Workshop on Induced Polarization. Rutgers University, New York (poster)

Izumoto, S., J. A. Huisman, E. Zimmermann, Y. Méheust, F. Gomez, J. Heyman, Y. Wu, H. Vereecken and T. Le Borgne (2018) Spectral induced polarization of calcite precipitation in a porous media. American Geophysical Union Fall Meeting. Washington, D.C. (poster)

Izumoto, S., J. A. Huisman, E. Zimmermann, O. Esser, F. -H Haegel and H. Vereecken (2018) Effects of solution composition on the spectral induced polarization signals of calcite precipitation. 4th Cargèse Summer School. Cargèse, Corsica (poster)

Izumoto, S., J. A. Huisman, Y. Wu and H. Vereecken (2019) Effect of solute concentration on the spectral induced polarization response of calcite precipitation. Geophysical Journal International (Accepted)

Klotzsche, A., Haruzi, P., Zhou, Z., Schmäck, J., Hoffmann, R., Vanderborght, J., Vereecken, H. and van der Kruk, J. (2019) High resolution characterization of time-lapse tracer experiments using crosshole GPR full-waveform inversion: Synthetic and field studies. American Geophysical Union Fall Meeting. San Francisco, CA. (oral)

Selles, A., R. Hoffmann, W. Uddin, P. Goderniaux, A. Dassargues, J.-C. Maréchal, and V. Tiwari (2019) Smart temperature tracing using heat and cold water in India. (Video of fieldwork during ENIGMA ITN secondment). <https://www.youtube.com/watch?v=cx6s4cGj1sc>

Short video clip planned to be published through Enigma social media about the heat tracer test at FZ Jülich.

Activities/Experimental campaigns/Monitoring

1. Already done experimental campaigns or monitoring

ESR9 Experimental plan	Dates	Site	Scientific Objectives	Participants	Datasets expected from the experiment & format
Experiment 1	5/2018-9/2018	Laboratory	Investigate electrical conductivity signature from saline diffusion		Electrical conductivity time-series and 2-D concentration field time-series
ESR12 Experimental plan	Dates	Site	Scientific Objectives	Participants	Datasets expected from the experiment & format
Experiment 1	19-30/3 2018	Laboratory	Investigate SIP response of calcite precipitation in a column setup		SIP responses
Experiment 2	14-21/8 2019	Laboratory	Investigate SIP response of calcite precipitation in a 2D measurement setup	CNRS Rennes	SIP responses, Images of calcite precipitations

	Dates	Site	Scientific Objectives	Participants	Datasets expected from the experiment & format
ESR10					
Experimental plan					
Experiment 1	29.4-13.5.19	Krauthausen	Test the potential of GPR FWI to reconstruct salt tracer plume	AQUALE (measurement equipment)	Time-lapse crosshole GPR FWI datasets; electrical conductivity data measured in boreholes.
Experiment 2	26.6-24.7.19	Krauthausen	Test the potential of GPR FWI to detect heat tracer	ESR6, ESR11, AQUALE (measurement equipment)	Time-lapse crosshole GPR FWI datasets; borehole temperature data.
ESR11					
Experimental plan					
Experiment 1	April 2018	Pic et Plat site (Chalk Mons, Belgium)	Heterogeneity characterization using as smart tracer artificial dissolved gases and heat jointly with a dye tracer	ULiege, UMon, Rennes 1 University	Time series of temperature and concentration data (breakthrough curve), Optical imaging, Logging, sampling
Experiment 2	November 2018, March 2019, April 2019, August 2019	Hyderabad test site India (BRGM and NGRI)	Processed based imaging using hot and cold water in a weathered granite aquifer system having a natural groundwater background temperature of 30 °C	ULiege, UMon, BRGM, (NGRI-Indian cooperation partner)	Time series of temperature and concentration data (breakthrough curve), optical imaging, logging, sampling
Complementing Experiment	June 2019	Krauthausen (FZ Jülich Germany)	Complementing a GPR survey imaging a heat tracer with a hot water injection	FZ Jülich (leader) ULiege, Rennes 1 University	Times series of temperature data (Breakthroughcurve), GPR observations of tracer movement
Monitoring	November 2018 to August 2019	Hyderabad test site India	Assistance at basic measurements performed by the BRGM team, e.g.	BRGM, (NGRI – Indian cooperation partner)	Temperature data with depth and water levels

water level
 measurements and
 temperature profiling
 (prerequisite for the
 tracer tests)

2. Planned experimental campaigns or monitoring

ESR9 Experimental plan	Dates	Site	Scientific Objectives	Participants	Datasets expected from the experiment & format
Experiment*	10/ 2019- 11/ 2019	Laboratory experiment at University of Rennes 1, Rennes.	Study the electrical potential signature from the saltwater intrusion in the context of a coastal aquifer	with ESR1	-Photographs of concentration fields (.png lossless compression format) -Time-series of electrical potential (ascii format)

ESR10 Experimental plan	Dates	Site	Scientific Objectives	Participants	Datasets expected from the experiment & format
Experiment*	2020	Krauthausen	Test the potential of GPR FWI to reconstruct desalinated tracer plume		Time-lapse crosshole GPR FWI datasets; electrical conductivity data in boreholes.
Experiment*	2020	Krauthausen	Test the potential of GPR FWI to reconstruct ethanol tracer plume		Time-lapse crosshole GPR FWI datasets

* These experiments are optional. Papers related to their results will be published after the end of the Enigma project.

ESR12 Experimental plan	Dates	Site	Scientific Objectives	Participants	Datasets expected from the experiment & format
Experiment 1	29 Oct. – 15 Nov.	Laboratory	To test the potential of newly developed 2D cell	CNRS Rennes	SIP responses, Images of bacteria

2019			for SIP response of bacteria growth		
Experiment 2	February 2020	Laboratory	To test the potential of newly developed 2D cell for SIP response of biotic mineral precipitation	CNRS Rennes	SIP responses, images of bacteria and precipitation

ESR11 has finished his experimental activities within the framework of ENIGMA.

Actual and expected scientific outputs

- A paper on the ability to use transversal and horizontal equivalent electrical conductivity time-series to constrain geostatistical models of hydraulic conductivity
- A paper or technical report on a geophysically-monitored tracer test to observe the signature of tracer diffusion on the apparent conductivity time-series
- A paper on the modeling of the horizontal and transversal equivalent conductivity time-series from the evolution of heterogeneous and/or non-stationary saline concentration fields
- A paper on the effect of solute concentration on the spectral induced polarization response of calcite precipitation (submitted)
- A paper on a newly developed measurement setup for monitoring the spectral induced polarization response of biochemical reaction
- A paper on the relationship between the spectral induced polarization response and development of calcite precipitation
- A possible paper on the simulation of calcite precipitation and spectral induced polarization responses using OpenFOAM
- A possible paper on the spectral induced polarization response of growing bacteria
- A paper on time-lapse ground penetrating radar full-waveform inversion to detect tracer plumes, a numerical study
- A paper on time-lapse ground penetrating radar full-waveform monitoring of a saline tracer
- A paper on time-lapse ground penetrating radar full-waveform monitoring of a heat tracer
- A paper on differences and complementarity of solute, heat and dissolved gas information for describing and imaging solute and heat transport in a complex dual porosity chalk aquifer
- A paper on interpretation and modeling of cold water injections in fractured rock (India) will be prepared with emphasis on density and viscosity effects
- A paper on heterogeneity and prior uncertainty investigation using a joint heat and solute tracer experiment in alluvial sediments is already published: Hoffmann, R., Dassargues, A., Goderniaux, P. and Hermans, T. (2019). Heterogeneity and prior uncertainty investigation using a joint heat and solute tracer experiment in alluvial sediments. *Frontiers in Earth Science – Hydrosphere*: **7** (108). doi: 10.3389/feart.2019.00108
- A paper on the effect of solute concentration on SIP response of calcite precipitation is already accepted: Izumoto, S., J. A. Huisman, Y. Wu and H. Vereecken (2019) Effect of solute concentration on the spectral induced polarization response of calcite precipitation. *Geophysical Journal International* (Accepted)

Expected joint scientific publications

- The paper on time-lapse ground penetrating radar full-waveform monitoring of a heat tracer will be co-authored by ESR6, ESR10 and ESR11 (lead author: Peleg Haruzi).
- ESRs 9-12 and ESR1 are currently exploring a short review paper focusing on process-based imaging. An outline of the manuscript has been made and a decision will soon be made to see if this review will be written or not.

- The various ESRs collaborate with the host institutions for the secondments. This implies that many of the final papers will have authors with two or more partners. Above, we focused only on planned papers involving multiple ESRs.

Data archiving and dissemination

ESR	Sites	Data types	Database	Contact person for the database	Format
ESR9	Laboratory	High-resolution photographs of 2-D concentration fields Time-lapse electrical conductivity data	H+ database		Uncompressed .tif figures and -ascii files
ESR10	Krauthausen	Time-lapse GPR Time-lapse electrical conductivity data Time-lapse temperature data	Tereno	Dr. Ralf Kunkel r.kunkel@fz-juelich.de	binary files xls files
ESR11	Hermalle-sous-Argenteau	Temperature and concentration time series, ERT profiles and hydrochemistry	H+ Database	Jerome de la Bernardie (University of Rennes 1) jerome.delabernardie@univ-rennes1.fr	.dat
	Pic et Plat	Temperature and concentration time series	H+ Database	Jerome de la Bernardie (University of Rennes 1)	.dat
	Hyderabad	Temperature and concentration time series	H+ Database	Jerome de la Bernardie, BRGM and Indo French Center for Groundwater Research in Hyderabad, India	.dat
ESR12	Laboratory	SIP measurements Images	Link from ENIGMA website (on-	Patricia Gautier (University of Rennes 1) (Temporary) patricia.gautier@univ-	.tif .mat

going) rennes1.fr

References

- Abdel Aal, G. Z., Slater, L.D., & Atekwana, E.A. (2006), Induced-polarization measurements on unconsolidated sediments from a site of active hydrocarbon biodegradation. *Geophysics* 71: H13–H24.
- Abdel Aal, G. Z., Atekwana, E. A., & Atekwana, E.A. (2010), Effect of bioclogging in porous media on complex conductivity signatures. *Journal of Geophysical Research* 115: 1–10.
- Abdel Aal, G. Z., Atekwana, E.A., Slater, L.D., & Atekwana, E.A. (2004), Effects of microbial processes on electrolytic and interfacial electrical properties of unconsolidated sediments. *Geophysical Research Letters* 31: L12505.
- Anderson, M.P. (2005), Heat as a ground water tracer. *Ground Water* 43: 951–968.
- Asnaashari, A., Brossier, R., Garambois, S., Audebert, F., Thore, P., & Virieux, J. (2015), Time-lapse seismic imaging using regularized full-waveform inversion with a prior model: which strategy? *Geophysical prospecting* 63: 78-98.
- Archie, G. E. (1942), The electrical resistivity log as an aid in determining some reservoir characteristics. *Transactions of the AIME* 146: 54-62.
- Benz, S.A., Bayer, P., & Blum, P. (2017), Global patterns of shallow groundwater temperatures. *Environmental Research Letters* 12: 034005.
- Binley, A., Hubbard, S.S., Huisman, J.A., Revil, A., Robinson, D.A., Singha, K., & Slater, L.D. (2015), The emergence of hydrogeophysics for improved understanding of subsurface processes over multiple scales. *Water Resources Research* 51: 3837–3886.
- Briggs, M.A., Day-Lewis, F.D., Ong, J.B.T., Curtis, G.P., & Lane, J.W. (2013), Simultaneous estimation of local-scale and flow path-scale dual-domain mass transfer parameters using geoelectrical monitoring. *Water Resources Research* 49: 5615-5630.
- Briggs, M.A., Day-Lewis, F.D., Ong, J.B.T., Harvey, J.W., & Lane, J.W. (2014), Dual-domain mass-transfer parameters from electrical hysteresis: Theory and analytical approach applied to laboratory, synthetic streambed, and groundwater experiments. *Water Resources Research* 50: 8281-8299.
- Bodin, J., Delay, F. & de Marsily, G. (2003), Solute transport in a single fracture with negligible matrix permeability: 1. Fundamental mechanisms. *Hydrogeology Journal* 11: 418–433.
- Brennwald, M.S., Schmidt, M., Oser, J., & Kipfer, R. (2016), A portable and autonomous mass spectrometric system for on-site environmental gas analysis. *Environmental Science & Technology* 50: 13455–13463.

Cassiani, G., Bruno, V., Villa, A., Fusi, N., & Binley, A.M. (2006), A saline tracer test monitored via time-lapse surface electrical resistivity tomography. *Journal of Applied Geophysics* 59: 244-259.

Camporese, M., Cassiani, G., Deiana, R., & Salandin, P. (2011), Assessment of local hydraulic properties from electrical resistivity tomography monitoring of a three-dimensional synthetic tracer test experiment. *Water Resources Research* 47, W12508.

Chen, J., Hubbard, S.S., & Williams, K.H. (2013), Data-driven approach to identify field-scale biogeochemical transitions using geochemical and geophysical data and hidden Markov models : Development and application at a uranium-contaminated aquifer. *Water Resources Research* 49: 6412–6424.

Chiles, J.-P. & Delfiner, P. (2009), *Geostatistics: Modeling Spatial Uncertainty*. Vol. 497. John Wiley & Sons.

Chatton, E., Labasque, T., de La Bernardie, J., Guihéneuf, N., Bour, O., & Aquilina, L. (2017), Field continuous measurement of dissolved gases with a CF-MIMS: Applications to the physics and biogeochemistry of groundwater flow. *Environmental Science & Technology* 51: 846–854.

Day-Lewis, F. D. & Singha, K. (2008), Geoelectrical inference of mass transfer parameters using temporal moments, *Water Resources Research* 44: W05201.

Day-Lewis, F. D., Linde, N., Haggerty, R., Singha, K., & Briggs, M.A. (2017), Pore network modeling of the electrical signature of solute transport in dual- domain media, *Geophysical Research Letters* 44: 4908– 4916.

Davis, C. A., Atekwana, E., Atekwana, E., Slater, L. D., Rossbach, S., & Mormile, M. R. (2006), Microbial growth and biofilm formation in geologic media is detected with complex conductivity measurements. *Geophysical Research Letters* 33: 1–5.

de La Bernardie, J., Bour, O., Le Borgne, T., Guihéneuf, N., Chatton, E., Labasque, T., Le Lay, H. & Gerard, M.-F. (2018), Thermal attenuation and lag time in fractured rock: Theory and field measurements from joint heat and solute tracer tests. *Water Resources Research* 54: 10,053-10,075.

Doetsch, J., Linde, N., Vogt, T., Binley, A., & Green, A.G. (2012), Imaging and quantifying salt-tracer transport in a riparian groundwater system by means of 3D ERT monitoring. *Geophysics* 77: B207-B218.

Domenico, P.A. & Schwartz, F.W. (1998), *Physical and Chemical Hydrogeology*, 2nd Edition, 2nd ed. John Wiley & Sons Inc., New York.

Flores Orozco, A., Williams, K. H., Long, P. E., Hubbard, S. S., & Kemna, A. (2011), Using complex resistivity imaging to infer biogeochemical processes associated with bioremediation of an uranium - contaminated aquifer. *Journal of Geophysical Research* 116: G03001.

Glaser, D. R., Werkema, D. D., Versteeg, R. J., Henderson, R. D., & Rucker, D. F. (2012), Temporal GPR imaging of an ethanol release within a laboratory-scaled sand tank. *Journal of Applied Geophysics* 86: 133-145.

Gregory, P. (2005), *Bayesian Logical Data Analysis for the Physical Sciences: A Comparative Approach with Mathematica® Support*. Cambridge University Press.

Gueting, N., Vienken, T., Klotzsche, A., van der Kruk, J., Vanderborght, J., Caers, J., Vereecken, H., & Englert, A. (2017), High resolution aquifer characterization using crosshole GPR full-waveform tomography: Comparison with direct-push and tracer test data. *Water Resources Research* 53: 49-72.

Hermans, T. (2017), Prediction-focused approaches: An opportunity for hydrology. *Groundwater* 55: 683–687.

Hubbard, C. G., West, L. J., Odriguez-Blanco, J. D., & Shaw, S. (2014), Laboratory study of spectral induced polarization responses of magnetite-Fe²⁺ redox reactions in porous media. *Geophysics* 79: D21–D30.

Irvine, D.J., Simmons, C.T., Werner, A.D. & Graf, T. (2015), Heat and solute tracers: How do they compare in heterogeneous aquifers? *Groundwater* 53: 10–20.

Jougnot, D., Jiménez-Martínez, J., Legendre, R., Le Borgne, T., Méheust, Y., & Linde, N. (2018), Impact of small-scale saline tracer heterogeneity on electrical resistivity monitoring in fully and partially saturated porous media: insights from geoelectrical milli-fluidic experiments. *Advances in Water Resources* 113: 295-309.

Kemna, A., Binley, A., Cassiani, G., Niederleithinger, E., Revil, A., Slater, L., Williams, K.H., Flores Orozco, A., Haegel, F.-H., Hördt, A., Kruschwitz, S., Leroux, V., Titov, K. & Zimmermann, E. (2012), An overview of the spectral induced polarization method for near-surface applications. *Near Surface Geophysics* 10: 453–468.

Kemna, A., Vanderborght, J., Kulesa, B., & Vereecken, H. (2002), Imaging and characterisation of subsurface solute transport using electrical resistivity tomography (ERT) and equivalent transport models. *Journal of Hydrology* 267: 125-146.

Klotzsche, A., van der Kruk, J., Meles, G. A., Doetsch, J., Maurer, H. & Linde, N. (2010). Full-waveform inversion of cross-hole ground-penetrating radar data to characterize a gravel aquifer close to the Thur River, Switzerland. *Near Surface Geophysics* 8: 635-649.

Klotzsche, A., Vereecken, H., & van der Kruk, J. (2019a), Review of crosshole GPR full-waveform inversion of experimental Data: Recent developments, challenges and pitfalls. *Geophysics* 84: 1-66.

Klotzsche, A., Vereecken, H., & van der Kruk, J. (2019b), GPR full-waveform inversion of a variably saturated soil-aquifer system. *Journal of Applied Geophysics* 170: 103823.

Koestel, J., Kemna, A., Javaux, M., Binley, A. & Vereecken, H. (2008), Quantitative imaging of solute transport in an unsaturated and undisturbed soil monolith with 3-D ERT and TDR. *Water Resources Research* 44: W12411.

Kurylyk, B.L. & Irvine, D.J. (2019), Heat: An overlooked tool in the practicing hydrogeologist's toolbox. *Groundwater* 57: 517–524.

Laloy, E., Linde, N., & Vrugt, J.A. (2012), Mass conservative three-dimensional water tracer distribution from Markov chain Monte Carlo inversion of time-lapse ground-penetrating radar data. *Water Resources Research* 48: W07510.

Maliva, R.G. (2016), *Aquifer Characterization Techniques*, Springer Hydrogeology. Springer International Publishing, Cham.

Maloszewski, P. & Zuber, A. (1993), Tracer experiments in fractured rocks: Matrix diffusion and the validity of models. *Water Resources Research* 29: 2723–2735.

Meigs, L.C. & Beauheim, R.L. (2001), Tracer tests in a fractured dolomite: 1. Experimental design and observed tracer recoveries. *Water Resources Research* 37: 1113–1128.

Mellage, A., Smeaton, C.M., Furman, A., Atekwana, E.A., Rezanezhad, F. & Cappellen, P. Van (2018), Linking spectral induced polarization (SIP) and subsurface microbial processes: Results from sand column incubation experiments. *Environmental Science & Technology* 52: 2081–2090.

Mewafy, F. M., Werkema Jr., D. D., Atekwana, E. A., Slater, L. D., Abdel Aal, G., Revil, A., & Ntarlagiannis, D. (2013), Evidence that bio-metallic mineral precipitation enhances the complex conductivity response at a hydrocarbon contaminated site. *Journal of Applied Geophysics* 98: 113–123.

Monego, M., Cassiani, G., Deiana, R., Putti, M., Passadore, G., & Altissimo, L. (2010), A tracer test in a shallow heterogeneous aquifer monitored via time-lapse surface electrical resistivity tomography. *Geophysics* 75: WA61-WA73.

Müller, K., Vanderborght, J., Englert, A., Kemna, A., Huisman, J. A., Rings, J., & Vereecken, H. (2010), Imaging and characterization of solute transport during two tracer tests in a shallow aquifer using electrical resistivity tomography and multilevel groundwater samplers. *Water Resources Research* 46: W03502.

Neretnieks, I., Eriksen, T. & Tähtinen, P. (1982), Tracer movement in a single fissure in granitic rock: Some experimental results and their interpretation. *Water Resources Research* 18: 849–858.

Noel, C., Gourry, J., Deparis, J., Ignatiadis, I., Battaglia-Brunet, F., & Guimbaud, C. (2016), Suitable real-time monitoring of the aerobic biodegradation of toluene in contaminated sand by spectral induced polarization measurements and CO₂ analyses. *Near Surface Geophysics* 14: 263–273.

Ntarlagiannis, D., Williams, K. H., Slater, L., & Hubbard, S. (2005), Low-frequency electrical response to microbial induced sulfide precipitation. *Journal of Geophysical Research* 110: G02009.

Ntarlagiannis, D., Yee, N., & Slater, L. (2005), On the low-frequency electrical polarization of bacterial cells in sands. *Geophysical Research Letters* 32: L24402.

Ntarlagiannis, D., Doherty, R., & Williams, K. H. (2010), Spectral induced polarization signatures of abiotic FeS precipitation. *Geophysics* 75: F127–F133.

Placencia-Gómez, E., Slater, L., Ntarlagiannis, D., & Binley, A. (2013), Laboratory SIP signatures associated with oxidation of disseminated metal sulfides. *Journal of Contaminant Hydrology* 148: 25–38.

Ptak, T., Piepenbrink, M. & Martac, E. (2004), Tracer tests for the investigation of heterogeneous porous media and stochastic modelling of flow and transport—a review of some recent developments. *Journal of Hydrology* 294: 122–163.

Read, T., Bour, O., Bense, V., Le Borgne, T., Goderniaux, P., Klepikova, M., Hochreutener, R., Lavenant, N. & Boscherio, V. (2013), Characterizing groundwater flow and heat transport in fractured rock using fiber-optic distributed temperature sensing. *Geophysical Research Letters* 40: 2055–2059.

- Reimus, P., Pohll, G., Mihevc, T., Chapman, J., Haga, M., Lyles, B., Kosinski, S., Niswonger, R. & Sanders, P. (2003), Testing and parameterizing a conceptual model for solute transport in a fractured granite using multiple tracers in a forced-gradient test: Multiple tracer testing in fractured rock. *Water Resources Research* 39:1356.
- Revil, A., Atekwana, E., Zhang, C., Jardani, A., & Smith, S. (2012), A new model for the spectral induced polarization signature of bacterial growth in porous media. *Water Resources Research* 48: W09545.
- Rubin, Y. (2003), *Applied Stochastic Hydrogeology*. Oxford University Press.
- Saneiyan, S., Ntarlagiannis, D., Werkema, D.D., & Ustra, A. (2018), Geophysical methods for monitoring soil stabilization processes. *Journal of Applied Geophysics* 148: 234–244.
- Sarris, T.S., Close, M. & Abraham, P. (2018), Using solute and heat tracers for aquifer characterization in a strongly heterogeneous alluvial aquifer. *Journal of Hydrology* 558: 55–71.
- Sen, P.N., Scala, C., & Cohen, M.H. (1981), A self-similar model for sedimentary rocks with application to the dielectric constant of fused glass beads. *Geophysics* 46: 781-795.
- Sen, P. N., & Goode, P. A., (1992), Influence of temperature on electrical conductivity on shaly sands. *Geophysics* 57: 89-96.
- Seyfried, M. S., & Grant, L. E. (2007), Temperature effects on soil dielectric properties measured at 50 MHz. *Vadose Zone Journal* 6: 759-765.
- Singha, K., & Gorelick, S.M. (2005), Saline tracer visualized with three-dimensional electrical resistivity tomography: Field-scale spatial moment analysis. *Water Resources Research* 41: W05023.
- Singha, K., Day-Lewis, F.D., & Lane Jr, J.W. (2007), Geoelectrical evidence of bicontinuum transport in groundwater, *Geophysical Research Letters* 34:L12401.
- Singha, K., Day-Lewis, F.D., Johnson, T., & Slater, L.D. (2015), Advances in interpretation of subsurface processes with time-lapse electrical imaging. *Hydrological Processes* 29: 1549-1576.
- Slater, L.D., Ntarlagiannis, D., & Wishart, D. (2006), On the relationship between induced polarization and surface area in metal-sand and clay-sand mixtures. *Geophysics* 71: A1–A5.
- Slater, L.D., Choi, J., & Wu, Y. (2005), Electrical properties of iron-sand columns: Implications for induced polarization investigation and performance monitoring of iron-wall barriers. *Geophysics* 70: G87–G94.
- Slater, L., Ntarlagiannis, D., Personna, Y. R., & Hubbard, S. (2007), Pore-scale spectral induced polarization signatures associated with FeS biomineral transformations. *Geophysical Research Letters* 34: L21404.
- Swanson, R.D., Singha, K., Day-Lewis, F.D., Binley, A., Keating, K., & Haggerty, R. (2012), Direct geoelectrical evidence of mass transfer at the laboratory scale. *Water Resources Research* 48:W10543.
- Tsang, C.-F. & Neretnieks, I. (1998), Flow channeling in heterogeneous fractured rocks. *Reviews of Geophysics* 36: 275–298.

Vanderborght, J., Kemna, A., Hardelauf, H., & Vereecken, H. (2005), Potential of electrical resistivity tomography to infer aquifer transport characteristics from tracer studies: A synthetic case study, *Water Resources Research* 41: W06013.

Vereecken, H., Döring, U., Hardelauf, H., Jaekel, U., Hashagen, U., Neuendorf, O., Jaekel, U., Hashagen, U., Neuendorf, O., Schwarze, H. & Seidemann, R. (2000), Analysis of solute transport in a heterogeneous aquifer: the Krauthausen field experiment. *Journal of Contaminant Hydrology* 45: 329-358.

Wildemeersch, S., Jamin, P., Orban, P., Hermans, T., Klepikova, M., Nguyen, F., Brouyère, S., & Dassargues, A. (2014), Coupling heat and chemical tracer experiments for estimating heat transfer parameters in shallow alluvial aquifers. *Journal of Contaminant Hydrology* 169: 90–99.

Wu, Y., Hubbard, S., Williams, K.H., & Ajo-Franklin, J. (2010), On the complex conductivity signatures of calcite precipitation. *Journal of Geophysical Research: Biogeosciences* 115: G00G04.

Wu, Y., Slater, L.D., & Korte, N. (2005), Effect of precipitation on low frequency electrical properties of zerovalent iron columns. *Environmental Science & Technology* 39: 9197–9204.

Wu, Y., Ajo-Franklin, J.B., Spycher, N., Hubbard, S.S., Zhang, G., Williams, K.H., Taylor, J., Fujita, A., & Smith, R. (2011), Geophysical monitoring and reactive transport modeling of ureolytically-driven calcium carbonate precipitation. *Geochemical Transactions* 12: 7.

Zhang, C., Slater, L., Redden, G., Fujita, Y., Johnson, T., & Fox, D. (2012), Spectral induced polarization signatures of hydroxide adsorption and mineral precipitation in porous media. *Environmental Science & Technology* 46, 4357–4364.

Zhang, C., Revil, A., Fujita, Y., Munakata-Marr, J., & Redden, G. (2014), Quadrature conductivity: A quantitative indicator of bacterial abundance in porous media. *Geophysics* 79: D363-D375.

End of deliverable WP4 D4.3 D11



Enigma ITN

WP4 D4.3 / D11